

**Microbial community productivity and diversity as responses to pH oscillation frequency**

Alice Carter  
Northwestern University  
1918 Sheridan Road, Evanston, IL 60208

Advisor: Dr. Joe Vallino  
Marine Biological Laboratory  
7 MBL Street, Woods Hole, MA 02543

Collaborator: George Allen  
Oberlin College  
101 North Professor Street, Oberlin OH, 44074

Semester in Environmental Science  
Independent Project, 2010

## Abstract

This experiment is an application of the intermediate disturbance hypothesis and the hypothesis that the productivity of a system increases as disturbance frequency decreases. As my avenue into these theories, I tested the response of seawater microbial communities to different frequencies of pH oscillation ranging from  $0 \text{ d}^{-1}$  to  $\frac{1}{2} \text{ d}^{-1}$ . I set up twelve 500 mL microcosms and maintained them as pulsed chemostats for 11 days with a sterile, nutrient enriched feed. Once the cultures had reached steady state I assessed productivity based on organic carbon concentrations in the efflux and *in situ* dissolved oxygen concentrations. I assessed diversity qualitatively by observing the steady state microbial communities with a DAPI stain under an epifluorescent microscope. Community productivity showed a negative quadratic relationship with pH oscillation frequency. I did not observe trends in level of diversity between the different frequency treatments though species morphology underwent a change as the frequency increased from  $0 \text{ d}^{-1}$  to  $\frac{1}{2} \text{ d}^{-1}$ .

## Keywords

diversity, productivity, intermediate disturbance, dissolved oxygen, microcosm, chemostat

## Introduction

A vast amount of genetic diversity is stored in the oceans; they contain a predicted  $3.6 \times 10^{29}$  microbial cells. Much of this genetic information can be found only in trace amounts in the system (Sogin et al 2006). With so many microbes, competitive exclusion by a few, well adapted species with high growth rates seems like it would occur readily, yielding a smaller, more homogenous metagenome (Hutchinson 1961). Many explanations of this seemingly paradoxical diversity exist. Hutchinson suggested that the variability present in natural ecosystems (fluctuations of environmental parameters,

seasonal changes, etc) prevents establishment of long term equilibrium conditions. When conditions shift, the system will be able to adapt by changing its species composition on the time scale of organism growth rate rather than waiting for the much slower time scale of evolution. If changes are rapid enough, the entire population in a system with only a few species could be wiped out long before they have the chance to evolve. Thus a system actually heightens its long-term productivity by preserving these trace genetic elements that may not be relevant to the current environmental parameters.

The intermediate disturbance hypothesis is one explanation of this point of view, stating that diversity will vary unimodally with disturbance frequency peaking at some intermediate level (Kassen et al. 2000). At low frequencies, environments would have time to reach near equilibrium conditions between disturbances. This leads to competitive exclusion by the most specialized, most productive organisms. Though the community productivity in this scenario remains high, the diversity declines drastically. At the other end of the spectrum, high frequencies of disturbance will lead to exclusion by adverse conditions due to fluctuations that are more rapid than the growth rates of the species. An intermediate disturbance frequency will moderate competitive exclusion without eliminating too many species by high frequency environmental change (Connell 1978, Scholes 2005).

Competitive exclusion only occurs when one organism's specific growth rate is greater than another's. This rate is evolutionarily maximized through an optimum production efficiency. At high efficiency, most of the carbon intake would go to biosynthesis, but it would occur at a very low reaction rate. At low efficiency even a very high reaction rate would not yield much biomass accumulation because most of the carbon would be lost to respiration (Vallino 2010). Therefore, maintaining metabolic functions at the optimum efficiency is of central importance to an organism because it will determine its ability to survive in a competitive environment. Striving of individual organisms to optimize efficiency yields a system that tends toward maximum productivity. This leads to the prediction that organisms will respond to disturbances in such a way to restore this balance and maintain high

production levels to the extent that they are capable. While the system is not disturbed too frequently, productivity remains high, indicating that the organisms can adapt quickly enough to hold their production efficiency near the optimum. As a system is placed under higher levels of stress more of its carbon intake is diverted from biomass production to maintenance energy requirements (Killham 1985). This shift is indicative of decreased stability and an inability of the organisms to maintain their production efficiencies, ultimately resulting in low net community productivity and therefore low diversity.

Experimental tests of these theories applied to microbial communities are small in number. Positive, negative and unimodal correlations of diversity and disturbance frequency have been documented in microbial mesocosms (Mittelbach et al 2001). The study described in this paper observes the effects of different frequencies of disturbance – in the form of continuous pH oscillations – on microbial diversity, biomass, productivity, and respiration in seawater microcosms.

## Methods

I set up and monitored 12 seawater microcosms. Each microcosm consisted of 500 mL of water kept in a liter Erlenmeyer flask. I collected the initial medium from stony beach approximately 10 m offshore and filtered it to 106 microns to remove large organisms that are heterogeneously distributed on the scale of 500 mL (Sheldon et al. 1972). I added nutrients to approximately 40 times ambient concentrations according to the Redfield Ratio; resulting concentrations were 40  $\mu\text{M}$   $\text{NH}_4\text{Cl}$ , 40  $\mu\text{M}$   $\text{Na}_2\text{SiO}_3$  and 2.5  $\mu\text{M}$   $\text{KH}_2\text{PO}_4$ . I incubated the cultures in a PGR15 Cenviron growth chamber at 15 °C with a 14/10 hr light/dark cycle under sodium and halide lamps emitting 1600 PAR. I allowed the cultures 9 days to acclimate before beginning to take samples.

I maintained the cultures as pulsed chemostats with a dilution rate of 30%  $\text{d}^{-1}$ . Every day I removed 150 mL from each flask, which I saved for various analyses, and replaced it with fresh, sterile

seawater. I obtained the replacement medium from the Marine Resource Center and filtered it with a 0.2  $\mu\text{m}$  filter cartridge (Gelman Sciences, Ann Arbor, MI). This added seawater contained a nutrient inoculum at the same concentrations I used in the initial cultures.

I adjusted the pH of each culture to a target value each day by adding a specific volume of 1 N HCL or 1 N NaOH. I assigned the volumes by experimentally determining the amount of acid or base required to move a 500 mL saline solution from a pH of 8 to 10 (700  $\mu\text{L}$  NaOH) or from 8 to 6 (600  $\mu\text{L}$  HCl). By multiplying these total volumes by their respective oscillation frequencies and correcting for acid or base removed during dilutions, I determined the required daily addition for each culture. My microcosms consisted of duplicates of six different frequency treatments; 0  $\text{d}^{-1}$ , 1/2  $\text{d}^{-1}$ , 1/4  $\text{d}^{-1}$ , 1/6  $\text{d}^{-1}$ , 1/8  $\text{d}^{-1}$ , and 1/10  $\text{d}^{-1}$  (figure 1).

With the 150 mL sample I removed from each microcosm I performed various analyses. I filtered 50 mL through a GF/F filter (Fisher Scientific, Fair Lawn, NJ) which I then placed in a desiccator containing 12 N HCL for 12 hours to remove the carbonates. After fumigation of the filters, I placed them in a 60 °C drying oven then analyzed them for carbon and nitrogen content with the Perkin Elmer CHNS10 Analyzer 2400.

I preserved 5 mL of the sample with gluteraldehyde for cell counts. I prepared slides by staining the cells with DAPI fluorescent stain and filtering the sample onto a 0.8  $\mu\text{m}$  polycarbonate filter which I observed with the Zeiss ImM#6 Axio Vision epifluorescent microscope under a fluorescent light (Porter 1980). I performed a qualitative diversity assessment for each sample by noting the differences in morphology and pigments of cells and the ratios in which different cells appeared.

I assessed nutrient uptake by measuring the nutrient concentrations of the samples removed from the microcosms. I analyzed phosphate, ammonium, and nitrate concentrations following the methods of Murphy and Riley 1962, Soloranzo 1969, and Wood et al. 1967 respectively. With an

additional portion of the sample I made an in-vivo fluorescence measurement of the chlorophyll a concentration using a Turner Designs 10-AU fluorometer.

To quantify bacterial productivity, I measured the rate of incorporation of  $^{14}\text{C}$ -labeled leucine into bacterial biomass by a freshly obtained sample. Following the method of Kirchman et al. 1993, I incubated the samples in 10 nM leucine, then compared the amount incorporated (measured using a Beckman Coulter LS-6500 scintillation counter) in a killed control and a sample after one hour of incubation. From this measurement, I used established conversion factors to calculate bacterial carbon incorporation.

To observe fluctuations in pH, dissolved oxygen, and temperature, I measured these parameters with a pH probe and a dissolved oxygen meter (Fischer Scientific, Fair Lawn, NJ). I took a measurement after pulsing each chemostat and at the beginning and end of each light and dark cycle. After accounting for fluctuation caused by diffusion, the remaining change in D.O. over time can be attributed to biological processes. Equation 1 describes this relationship, where  $k$  is an experimentally determined diffusion constant for oxygen,  $C_{\text{sat}}(t)$  is the saturated D.O. concentration when the water is at equilibrium with the air,  $C(t)$  is the actual D.O. concentration in the water, and  $R_{\text{O}_2}$  is the D.O. change caused by organisms.  $C_{\text{sat}}$  was empirically determined from the temperature and salinity of the water following the equation derived by Weiss, 1970. To make  $C_{\text{sat}}(t)$  and  $C(t)$  functions of time, I assumed that they change linearly between the start and end points. To measure the oxygen diffusion coefficient, I set up Erlenmeyer flasks containing 500 mL of sterile seawater at 15 °C to be bubbled with nitrogen gas overnight to remove all dissolved oxygen. After turning off the  $\text{N}_2$  gas, I monitored the D.O. concentration every 15 minutes as it returned to equilibrium with the atmosphere. This generated an exponential function of time and of the diffusion coefficient  $k$  described by equation 2, which I solved for a  $k$  value to be used in equation 1.

## Results

The actual pH of each of the microcosms tracked well with the target pH after acid/base additions. The overall oscillations I achieved are shown in figure 1. In between pulsing the chemostats, the pH relaxed back toward 8 as carbon dioxide diffused in or out of the solution to reach equilibrium (figure 2). Nutrient concentrations were highly variable for the first part of the incubation period with ammonium concentrations ranging from 0 to 20  $\mu\text{M}$  and phosphate from 0 to 2.5  $\mu\text{M}$  across all the treatments. By the last three days of incubation the concentrations of both nutrients had stabilized with the ammonium and phosphate concentrations very low in most treatments, with significant amounts present in only the highest frequency ( $f=1/2 \text{ d}^{-1}$ ) treatment (figures 3, 4).

I measured the carbon concentration in samples removed from the cultures using a CHN analyzer at the beginning and the end of the incubation period. The initial cultures contained mostly uniform levels, averaging 300  $\mu\text{M C}$ . The final samples had differentiated to show a decreasing trend in productivity with increasing oscillation frequency (figure 5). Chlorophyll a concentrations increased over time and show a trend similar to that of carbon concentrations in their steady state values; decreasing as oscillation frequency increases (figures 7, 8).

Contrary to the transient productivity trends observed with the chlorophyll and carbon concentration data, bacterial productivity analysis using  $^{14}\text{C}$ -labeled leucine indicated that the productivity decreased over time in almost all of the cultures. The productivity on the final day however mirrored the decreasing trend across treatments with increasing oscillation frequency observed with the CHN data (figure 9).

Dissolved oxygen concentrations depicted clear diurnal cycles with  $\text{O}_2$  concentration rising during the day and falling at night. Solving equation 1 for  $R_{\text{O}_2}$  showed how much of the change in concentration could be attributed to biologically mediated processes with a positive value indicating net production and a negative value indicating net respiration. I used this data to calculate the net

community productivity and community respiration in each of the chemostats. The resulting values are shown in figure 11. By assuming the production and respiration remain constant over time and scaling the rate of net community production to the 14 hour light cycle and the community respiration rate to the entire 24 hours, I calculated gross primary production using equation 3. This indicator of primary production also follows a decreasing trend with increasing oscillation frequency (figure 12).

I assessed diversity of the different cultures by observing DAPI stained cells under fluorescent light. The initial cultures contained a wide array of species (with different species being identified based on morphology) including high concentrations of nanoflagellates and filamentous bacteria (figure 14). The species composition of all 12 of the microcosms changed significantly over the incubation period. Observable diversity declined and a single species of diatom became dominant suspended in the water while a filamentous multi-cellular algae was prevalent on the walls of the flasks (figure 15). Comparison between the 6 frequency treatments showed a decrease in chlorophyll a with higher frequencies, a loss of filamentous bacteria species with higher frequencies and a gradual change in diatom morphology (figures 16-19). Aside from these trends, I did not see a strong signal of difference in diversity level between the treatments.

## Discussion

Before analyzing my data, it is important that I confirm my driving variable followed the intended trends. Plotting the pH after daily acid/base addition against time indicates that the six different oscillation frequencies were achieved as desired (figure 1). Significant degassing took place in between these additions (i.e. figure 2). This can mostly be attributed to diffusion of CO<sub>2</sub> in and out of the solution as the carbonate buffer system comes back into equilibrium with the altered pH. Ammonium additions do not significantly contribute to the water's buffering capacity, nor does the NaOH addition appear to cause excessive volatilization of the ammonium – when I compared ammonium

concentrations to pH of the previous day, I observed no correlation. I did see indications that some of the buffering is biologically mediated. One of the two highest frequency treatments ( $f = \frac{1}{2} \text{ d}^{-1}$ ) experienced a sharp decline in organic carbon concentrations and productivity while the other did not. The less productive microcosm had only about 75% the buffering capacity of the more productive microcosm. Even accounting for this relaxation in pH extremes overnight, the overall cycles are unique enough to draw conclusions about their effects on the system.

My experiment is not concerned with temporal variation, rather it looks at differences between the steady states of systems that have been exposed to different conditions. Because of this, it was necessary to use chemostats rather than batch cultures and to ensure they had reached steady state before taking measurements for comparison between treatments. The best indicators that this state had been reached are the nutrient concentration changes over time. They undergo a change from sporadic, large fluctuations to relatively constant values around day 7 of the incubation (figures 3-4). Chlorophyll a concentrations also level out over time as steady state is approached (figure 7).

Because I added a sterile feed to my chemostats, any organic carbon present in the removed samples must have been produced in the chemostat. This allows for a straightforward assessment of net community productivity; it is proportional to the carbon concentrations measured in the efflux from the systems. Chlorophyll a concentrations are an indicator of primary productivity in the system. Both of these data show the predicted negative relationship between productivity and pH oscillation frequency (figures 6, 8). The chlorophyll a concentration is decreasing at a faster rate than the carbon concentration as the pH oscillation frequency increases, yielding a carbon to chlorophyll ratio that increases along with oscillation frequency. This increasing ratio may be indicative of increasing stress; the microbes in the highest frequency oscillation microcosm are allocating more of their carbon to maintenance and structure, leaving less available for chlorophyll. This agrees with the overall decrease in productivity as primary producers with lower chlorophyll content will be less productive.

Measures of net community production from concentrations of carbon suspended in the water are underestimates; this method ignores production on the walls of the chemostat (a development which this setup actually selects for because they don't get diluted with each pulse). Net community productivity can be more accurately assessed using diurnal fluctuations in dissolved oxygen. During the day, D.O. concentrations increase and at night they decrease, corresponding to net production and net respiration respectively (figure 9). Using equations 1 and 2 as described above, I accounted for the effects of oxygen diffusion and isolated the changes due to the biological community. As expected, these values are positive during the day and negative at night (figure 10). Plotting these calculated net community productivities against their proportionally spaced oscillation frequencies reveals a strong correlation to a negative second order polynomial decay curve (figure 11). The relatively constant respiration across the treatments indicates that the P/R ratio (a measure of efficiency) will follow the same trend as productivity; decreasing with increasing oscillation frequency. Using equation 3 with the assumptions outlined above, I calculated GPP for each frequency treatment. These values further corroborate the negative relationship between productivity and oscillation frequency.

Assessment of diversity trends was not as conclusive as that of productivity trends. There was a distinct decline in diversity from the initial samples over time. Though this is not a trend I was looking for it may still be an indicator of increasing diversity with decreasing disturbance. Even with my introduced disturbance of pH oscillation, the seawater microbial community had been moved from the ocean into a bottle where the temperature, nutrient and light levels were all held constant. Overall, this is a shift to a lower disturbance regime than the open ocean – possibly the cause of diversity loss. Comparison of DAPI stained slides from the different frequency treatments after they had reached steady state did not demonstrate the predicted unimodal peak in diversity. Some trends could be discerned such as decreasing chlorophyll a and cell density with increasing frequency, however these are merely confirmations of trends observed with other measurements. There is a shift in species composition and

morphology to more rounded diatoms and more filamentous bacteria as frequency decreases from  $\frac{1}{2} \text{ d}^{-1}$  to  $0 \text{ d}^{-1}$  (figures 16-19). This relationship does not indicate more or less diversity at either high or low frequencies rather just variation in species across treatments. Possibly a more quantitative measure of diversity would reveal subtle trends than I have not seen with my loose estimation.

All of the cultures have higher cell densities and are more of a diatom monoculture than they were at the beginning of the incubation period. This may be attributable to the high level of nutrient addition. Nutrient input is its own form of disturbance, and its effects seem to have overshadowed any effects of the different pH oscillation frequencies. To achieve higher resolution data on the comparison between treatments, I would either have to increase the intensity of the disturbance I want to observe (pH oscillation) or decrease the level of nutrient addition.

Even with these modifications, diversity is a difficult phenomena to cultivate in this setup. The cultures were very small and had a high degree of physical transport, preventing the formation of physical gradients and therefore differentiation of niches. There were only two distinct environments in my cultures: the walls of the flasks and the suspended medium. Both of these niches were dominated by a single species; the multicellular algae in figure 15 and the diatoms in figures 16-19 respectively. Increasing the cultures size or decreasing the physical transport (possibly through the use of a higher viscosity medium) would allow for a higher degree of diversification, probably yielding more discernable trends in diversity.

Though this experiment was an unsuccessful demonstration of the intermediate disturbance hypothesis in microbial microcosms, it has added to the knowledge on how to study disturbance in these systems. Adaptations to these methods in further studies have the potential to yield stronger results.

## Acknowledgements

I thank my advisor Dr. Joe Vallino for all of his guidance and advice throughout this project. Also, I thank my intellectual and methodological collaborator George Allen as well as the course TA's Rich McHorney, Will Daniels, and Stefanie Strebel and Ken Foreman for all of their assistance. This project was funded by the Semester in Environmental Science Program 2010 with lab space and equipment provided by the Marine Biological Laboratory.

## References

- Butler, G.J., and G.S.K. Wolkowicz. 1985. A Mathematical Model of the Chemostat with a General Class of Functions Describing Nutrient Uptake. *SIAM Journal of Applied Mathematics*, **45(1)**: 138-151.
- Connell, J.H. 1978. Diversity in Tropical Rain Forests and Coral Reefs. *Science*, **24**: 1302-1310.
- Hutchinson, G.E. 1961. The Paradox of the Plankton. *The American Naturalist*, **95(882)**: 137-145.
- Kassen, R., A. Buckling, G. Bell, and P.B. Rainey. 2000. Diversity peaks at intermediate productivity in a laboratory microcosm. *Letters to Nature*, **406**: 508-512.
- Killham, K. 1985. A Physiological Determination of the Impact of Environmental Stress on the Activity of Microbial Biomass. *Environmental Pollution (Series A)*, **38**: 283-294.
- Kirchman, D.L. 1993. Leucine Incorporation as a Measure of Biomass Production by Heterotrophic Bacteria. *Handbook of Methods in Aquatic Microbial Ecology*, P.F. Kemp, B.F. Sherr, E.B. Sherr, and J.J. Cole, Eds, Lewis Publishers :509-512.
- Mittelbach et al. 2001. What is the Observed Relationship Between Species Richness and Productivity? *Ecology*, **82(9)**: 2381-2396.
- Murphy J., J.P. Riley. 1962. A modified single solution method for the determination of phosphate in natural water. *Anal Chem. Acta* **27**: 31-36
- Porter, K.G. and Y.S. Feig. 1980. The use of DAPI for identifying and counting aquatic microflora.

- Limnology and Oceanography, **25(5)**: 948-951.
- Scholes, L., P.H. Warren, and A.P. Beckerman. 2005. The combined effects of energy and disturbance on species richness in protist microcosms. Ecology Letters, **8**: 730-738.
- Sheldon, R.W., A. Prakash, and W.H. Sutcliffe, Jr. 1972. The size distribution of particles in the ocean. Limnology and Oceanography, **17(3)**: 327-340.
- Sogin, M.L., H.G. Morrison, J.A. Huber, D.M. Welch, S.M. Huse, P.R. Neal, J.M. Arrieta, and G.J. Herndl. 2006. Microbial diversity in the deep sea and the underexplored "rare biosphere". Proceedings of the National Academy Sciences **103(32)**: 12115-12120.
- Soloranzo, L. 1969. Determination of ammonia in natural waters by the phenolhypochlorite method. Limnol. Oceanogr. **14**: 799.
- Vallino, J.J. 2010. Ecosystem biogeochemistry considered as a distributed metabolic network ordered by maximum entropy production. Philosophical Transactions of the Royal Society of Biological Sciences. **365(1545)**: 1417-1427.
- Weiss, R.F. 1970. The solubility of nitrogen, oxygen and argon in water and seawater. Deep Sea Research. **17**: 721-725.
- Wood, E.D., F.A.G. Armstrong, and F.A. Richards. 1967. Determination of nitrate in seawater by cadmium-copper reduction to nitrite. J.Mar. Biol. Assoc. U.K. **47**:23

## Equations

$$\frac{dC(t)}{dt} = k(C_{sat}(t) - C(t)) + R_{O_2} \quad (1)$$

$$C(t) = C_{sat}(1 - e^{-kt}) \quad (2)$$

$$GPP = NCP - R_C \quad (3)$$

## Figures and Tables

- Figure 1: pH after addition of acid or base in for each frequency treatment.
- Figure 2: pH curve for the frequency =  $\frac{1}{2} \text{ d}^{-1}$  treatment demonstrating the relaxation of pH in between acid and base addition due to the carbonate buffer system.
- Figure 3: Ammonium concentrations in the six different treatments through the duration of the incubation period.
- Figure 4: Phosphate concentrations in the six different treatments through the duration of the incubation period.
- Figure 5: Initial and final concentrations of carbon in the six different treatments measured using CHN analysis.
- Figure 6: Net Community Production calculated from CHN analysis of the steady state cultures plotted against pH oscillation frequency.
- Figure 7: Changes through time of chlorophyll a concentrations in each of the six frequency treatments.
- Figure 8: Chlorophyll a concentrations in the steady state cultures plotted against pH oscillation frequency.
- Figure 9: Bacterial productivity at the beginning of incubation, half way through the incubation period and in the steady state cultures at the end of the incubation period in all six of the pH oscillation frequency treatments.
- Figure 10: Diurnal cycles in dissolved oxygen concentrations in the six different frequency treatments during the last four days of the incubation period.
- Figure 11: Net Community Production and Community respiration rates from the final four days of incubation in the six different pH oscillation frequency treatments. Values were calculated from fluxes in dissolved oxygen and from an experimentally determined oxygen diffusion constant.
- Figure 12: Second order polynomial decay curve describing the relationship between net community productivity and pH oscillation frequency.
- Figure 13: Gross primary productivity measured over the final four days of incubation of the six pH oscillation frequency treatments. Values were calculated by scaling net community production to 14 hours and community respiration to 24 hours and subtracting respiration from NCP (equation 3).
- Figure 14: Fluorescent image of DAPI stained nanoflagellates and filamentous bacteria present in initial cultures (11/30).
- Figure 15: Fluorescent image of a multi-cellular filamentous algae species found on the walls of the cultures (12/11).
- Figure 16: Fluorescent image of cells from the  $0 \text{ d}^{-1}$  frequency treatment after it had reached steady state (12/11). This culture contained the most filamentous bacteria and the most chlorophyll a, seen in this auto-fluorescent image as red, of all the steady state

microcosms.

Figure 17: Fluorescent image of cells from the  $1/10 \text{ d}^{-1}$  frequency treatment after it had reached steady state (12/11).

Figure 18: Fluorescent image of cells from the  $1/6 \text{ d}^{-1}$  frequency treatment after it had reached steady state (12/11).

Figure 19: Fluorescent image of cells from the  $1/2 \text{ d}^{-1}$  frequency treatment after it had reached steady state (12/11). This culture contained the least chlorophyll a of all the steady state microcosms.

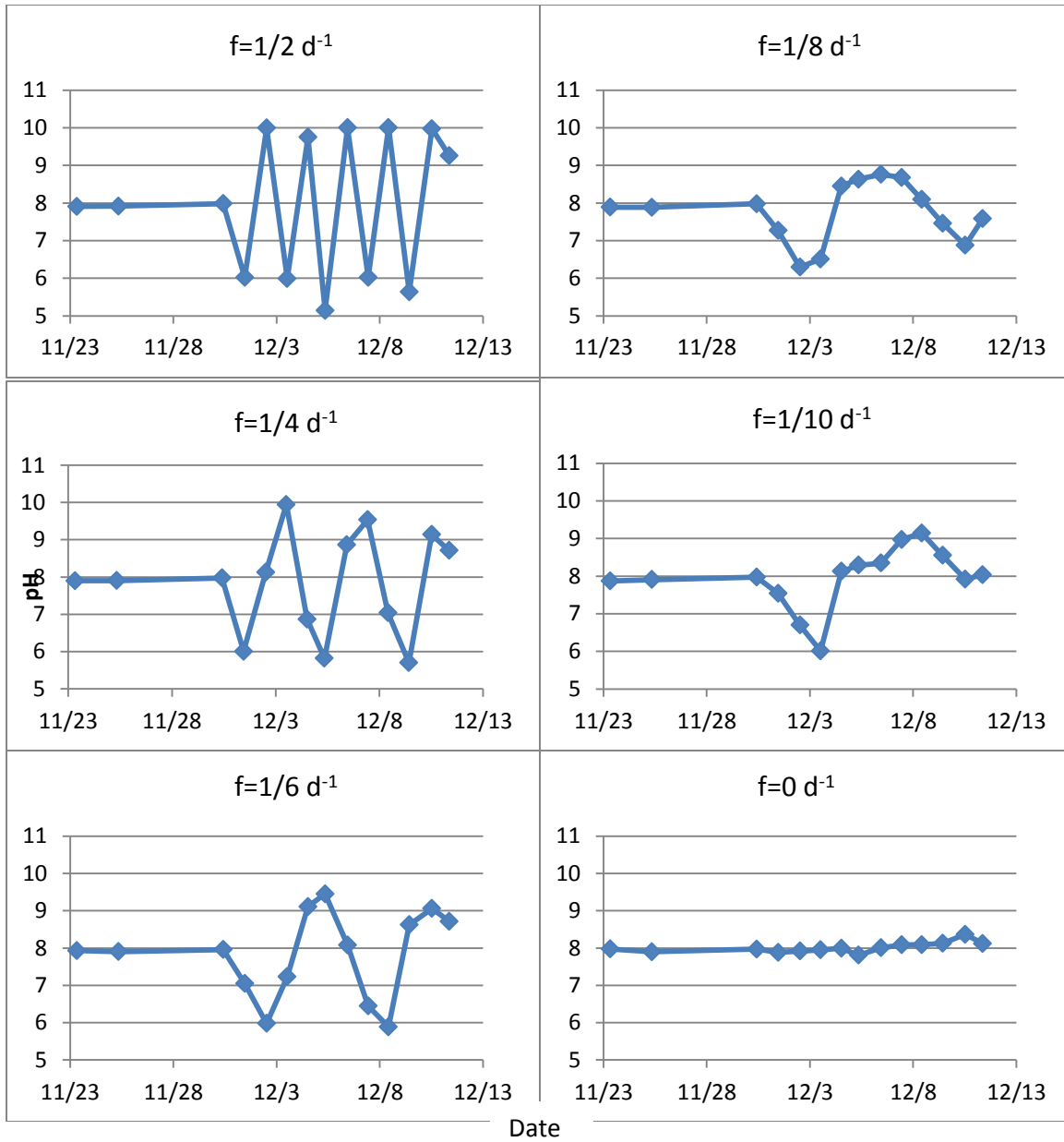
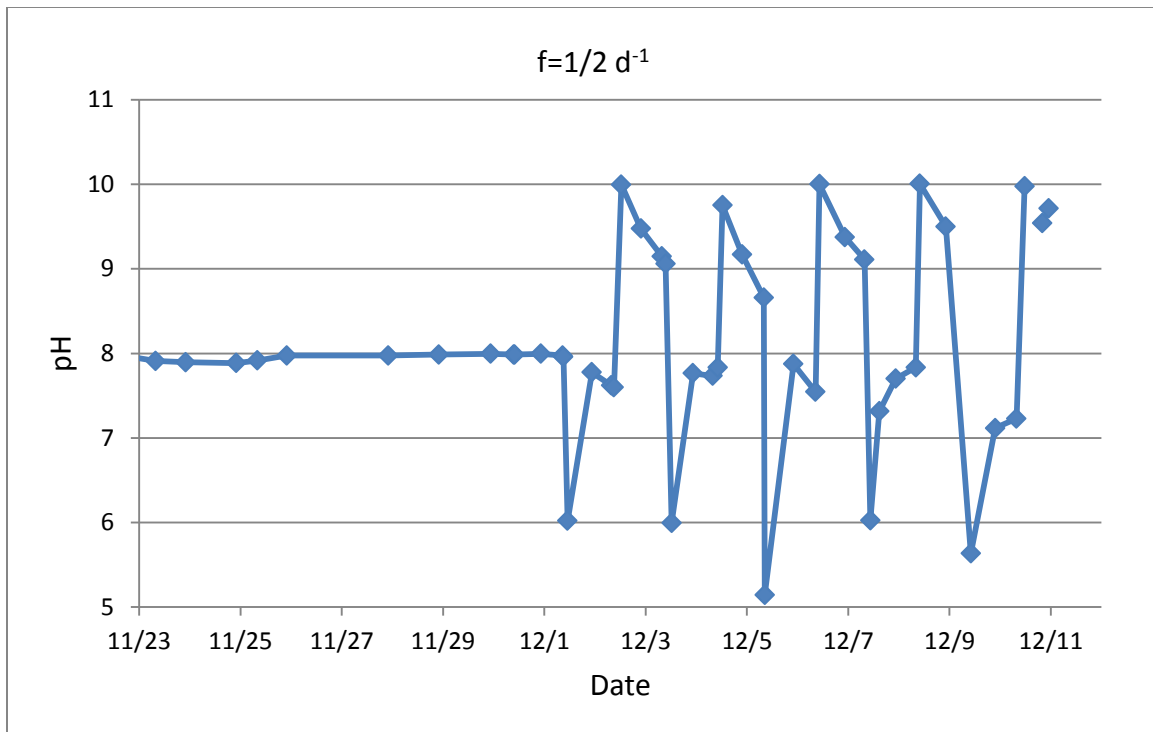


Figure 1: pH after addition of acid or base in for each frequency treatment.



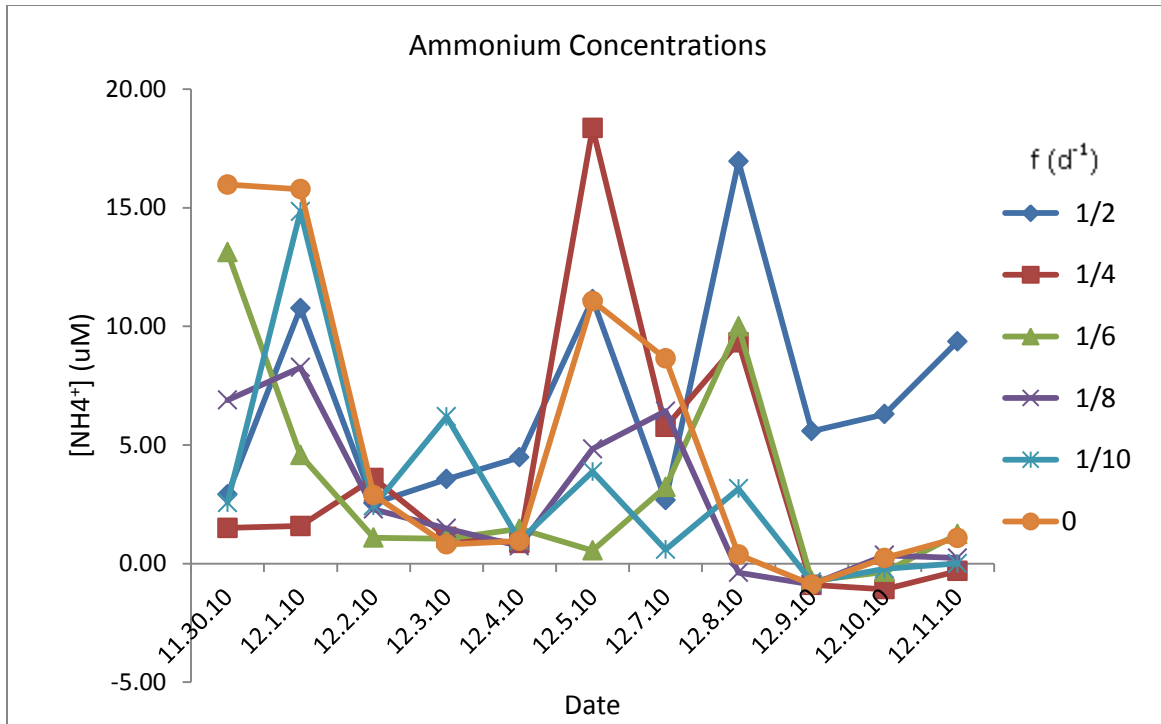


Figure 3: Ammonium concentrations in the six different treatments through the duration of the incubation period.

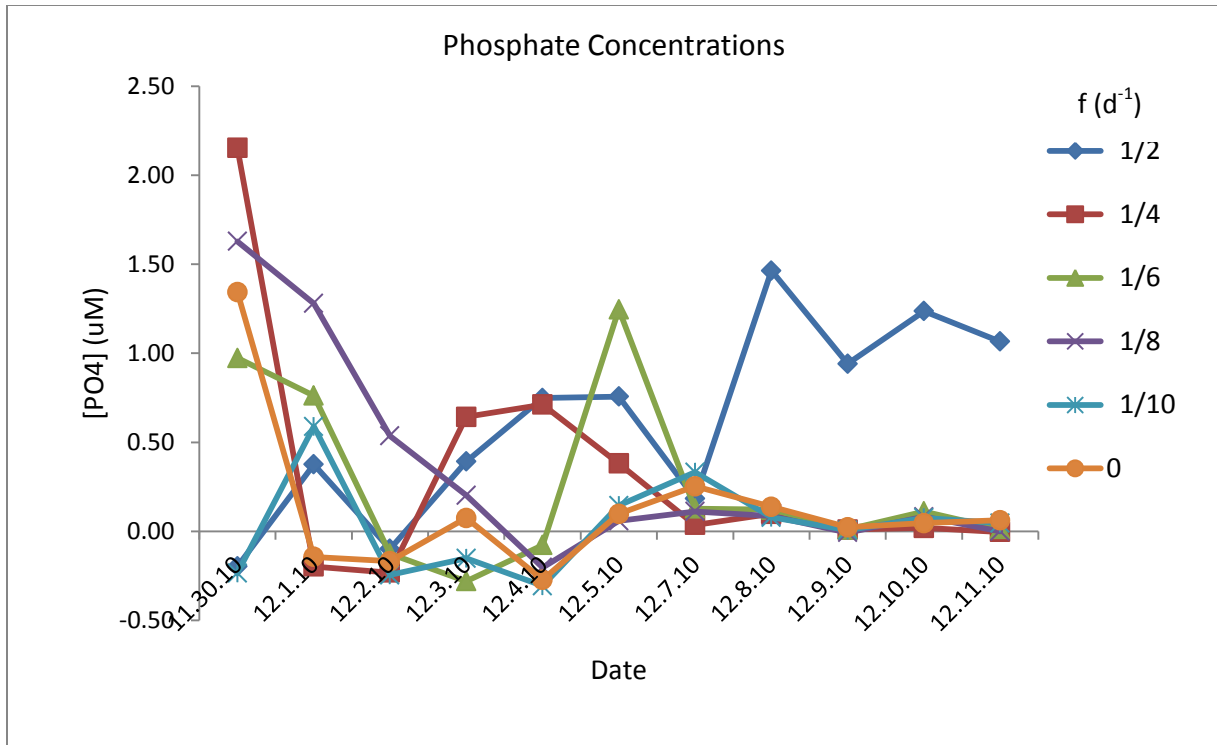


Figure 4: Phosphate concentrations in the six different treatments through the duration of the incubation period.

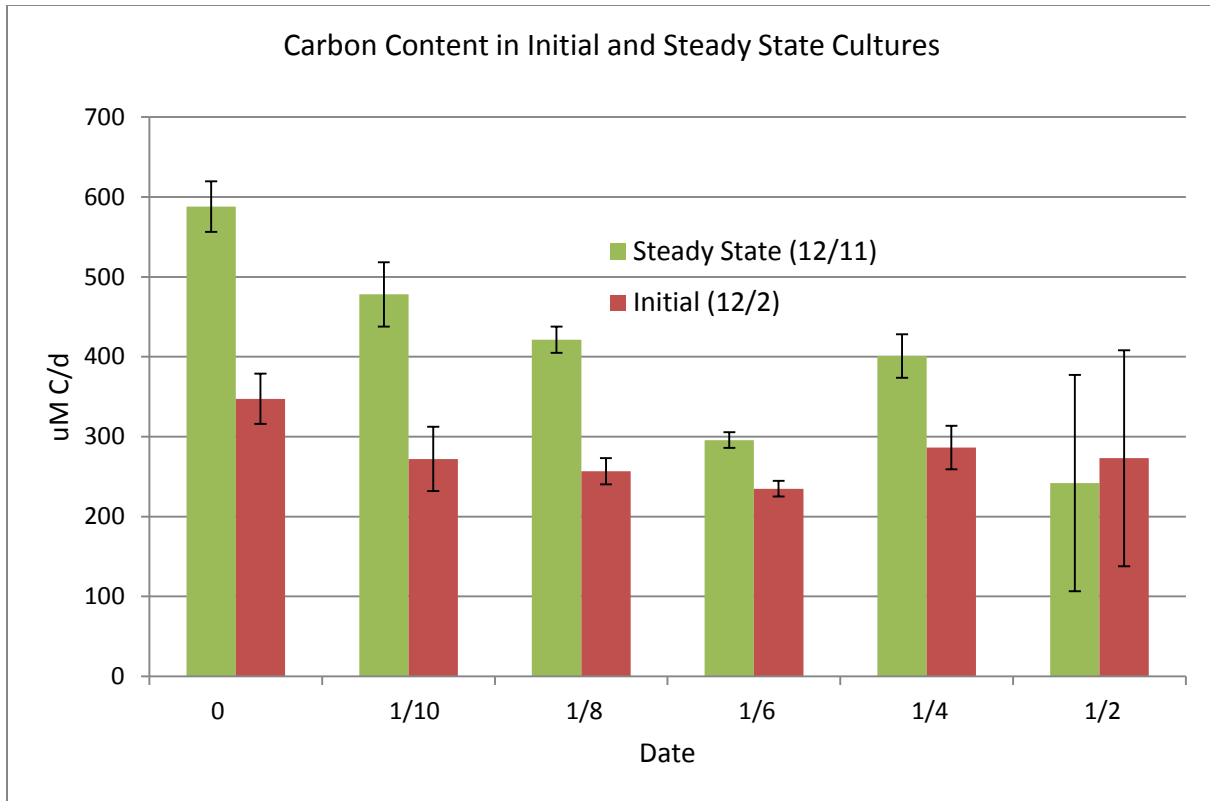


Figure 5: Initial and final concentrations of carbon in the six different treatments measured using CHN analysis.

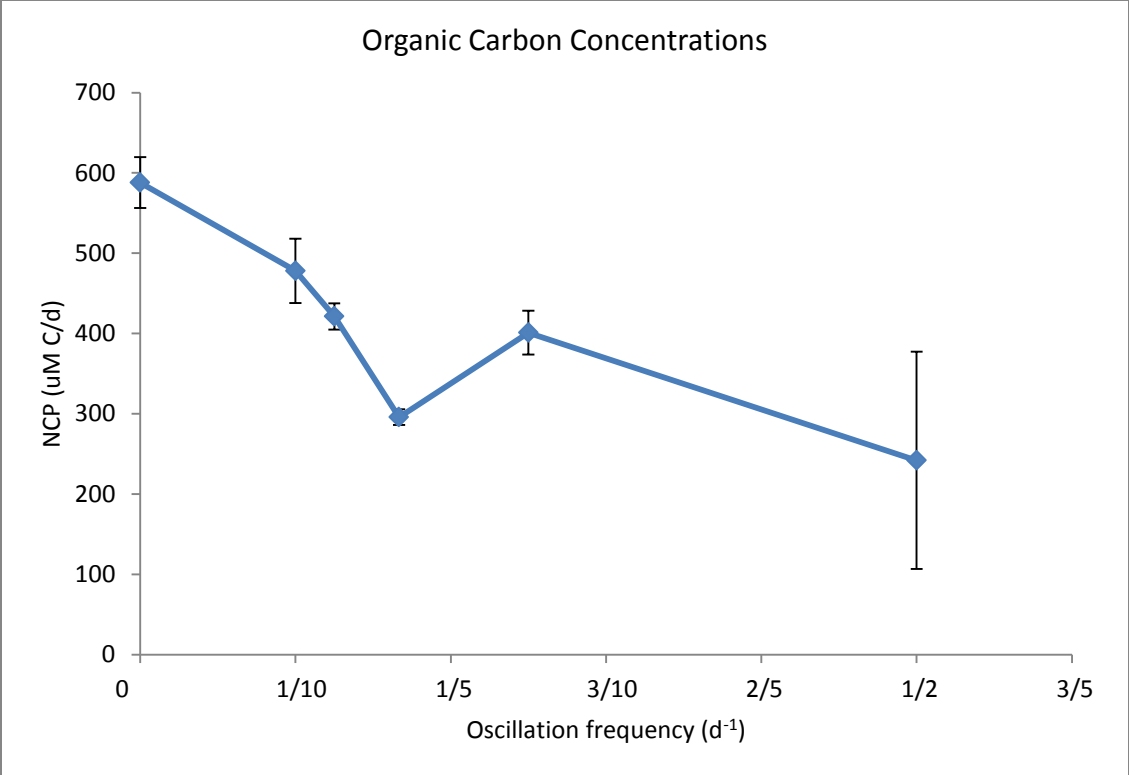


Figure 6: Net Community Production calculated from CHN analysis of the steady state cultures plotted against pH oscillation frequency.

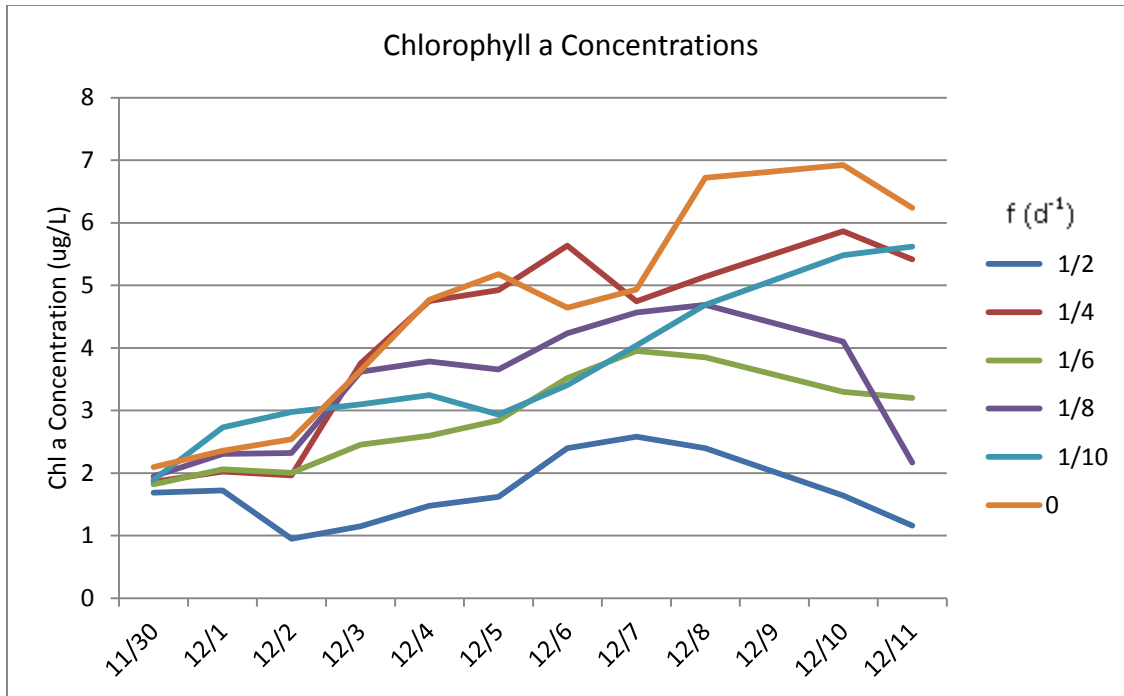


Figure 7: Changes through time of chlorophyll a concentrations in each of the six frequency treatments.

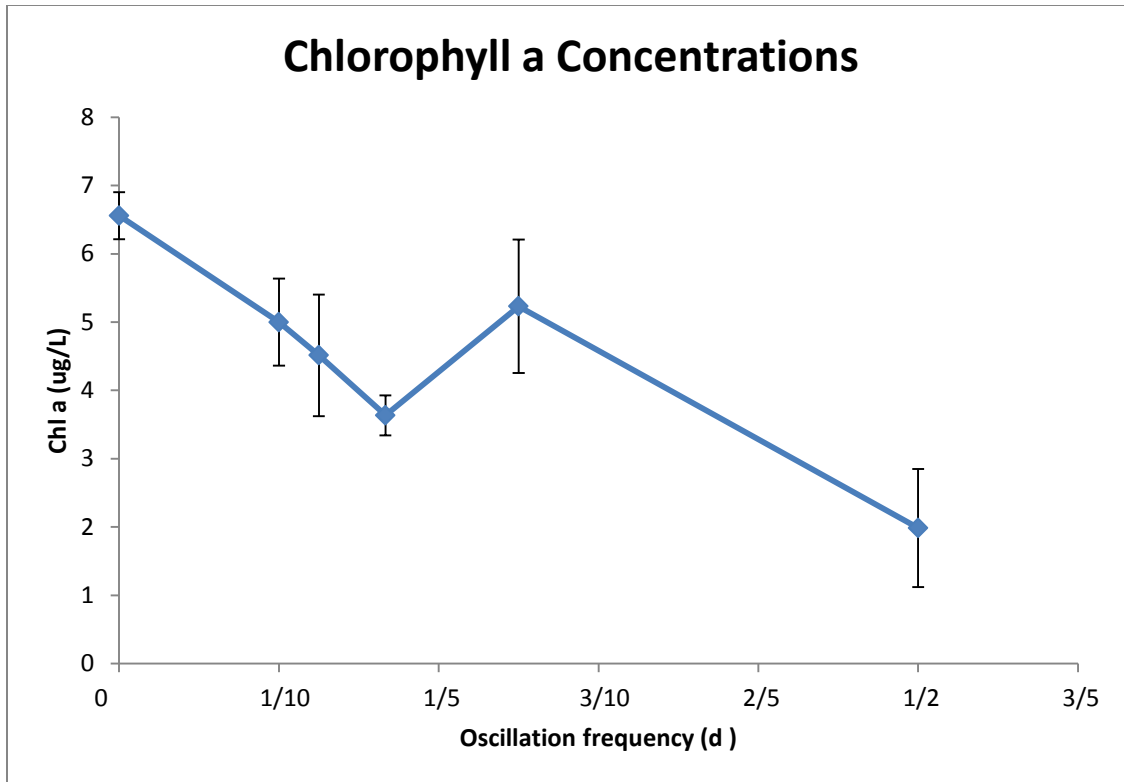


Figure 8: Chlorophyll a concentrations in the steady state cultures plotted against pH oscillation frequency.

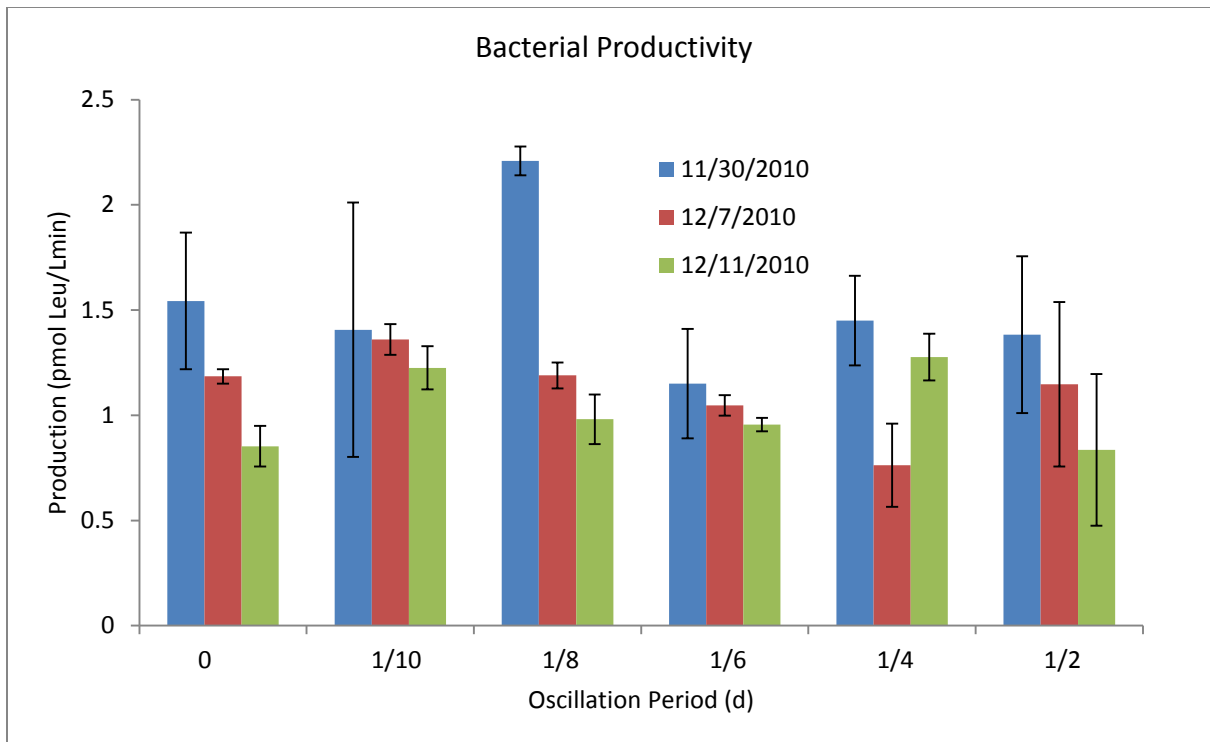


Figure 9: Bacterial productivity at the beginning of incubation, half way through the incubation period and in the steady state cultures at the end of the incubation period in all six of the pH oscillation frequency treatments.

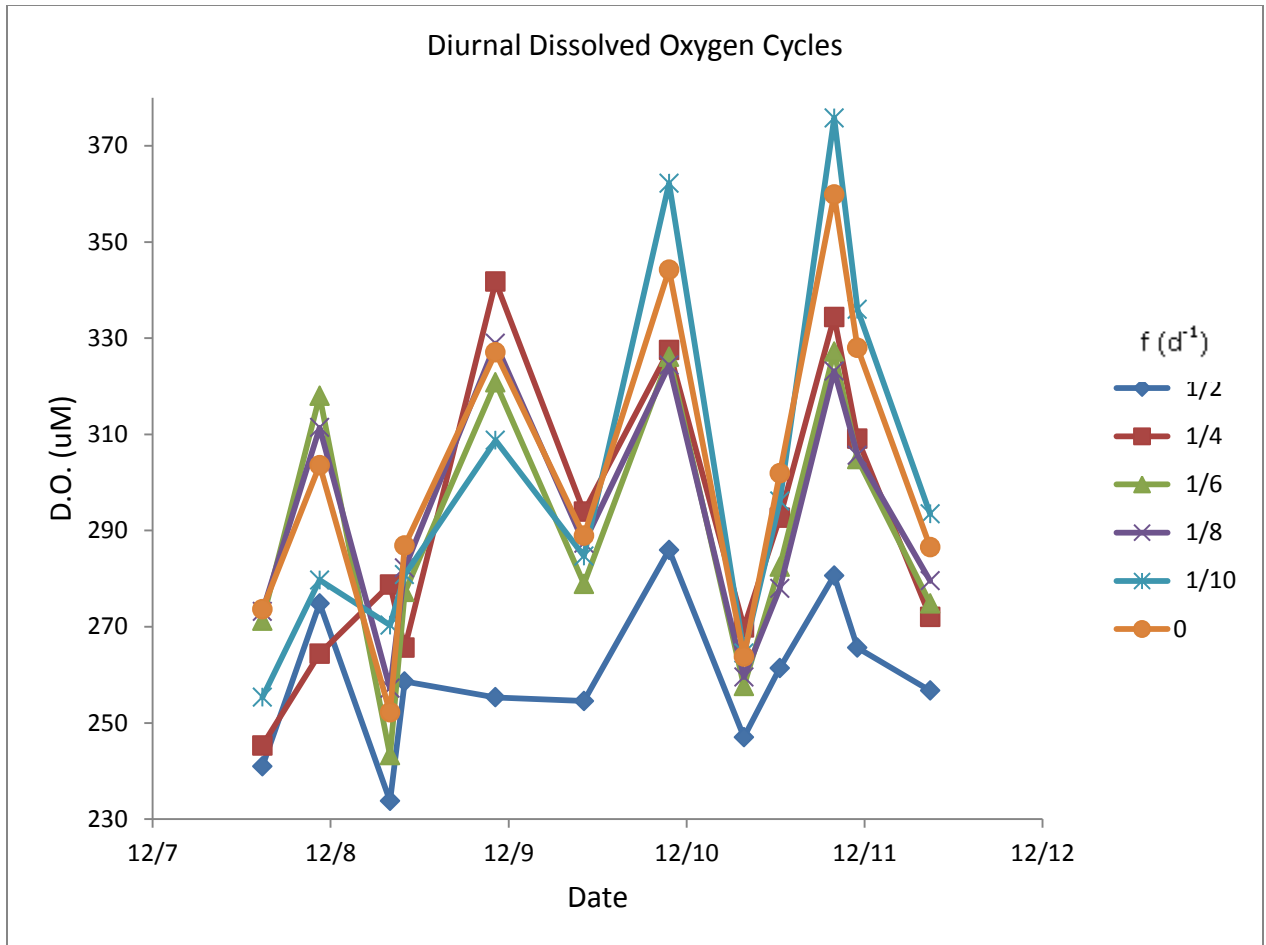


Figure 10: Diurnal cycles in dissolved oxygen concentrations in the six different frequency treatments during the last four days of the incubation period.

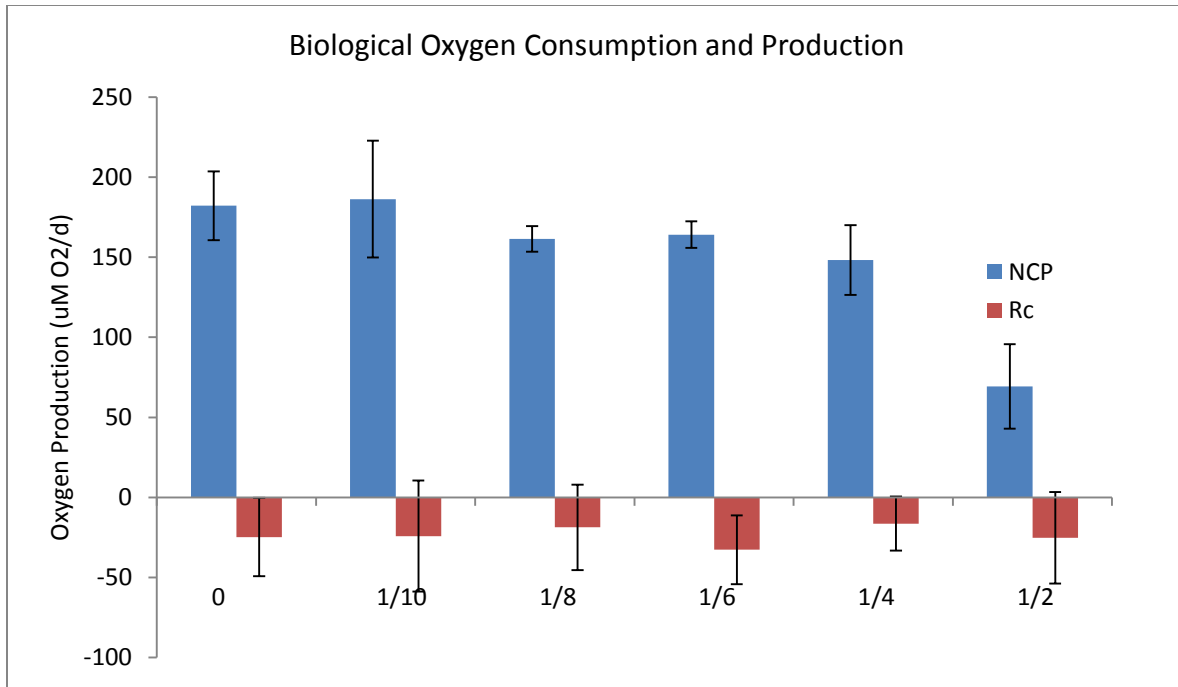


Figure 11: Net Community Production and Community respiration rates from the final four days of incubation in the six different pH oscillation frequency treatments. Values were calculated from fluxes in dissolved oxygen and from an experimentally determined oxygen diffusion constant.

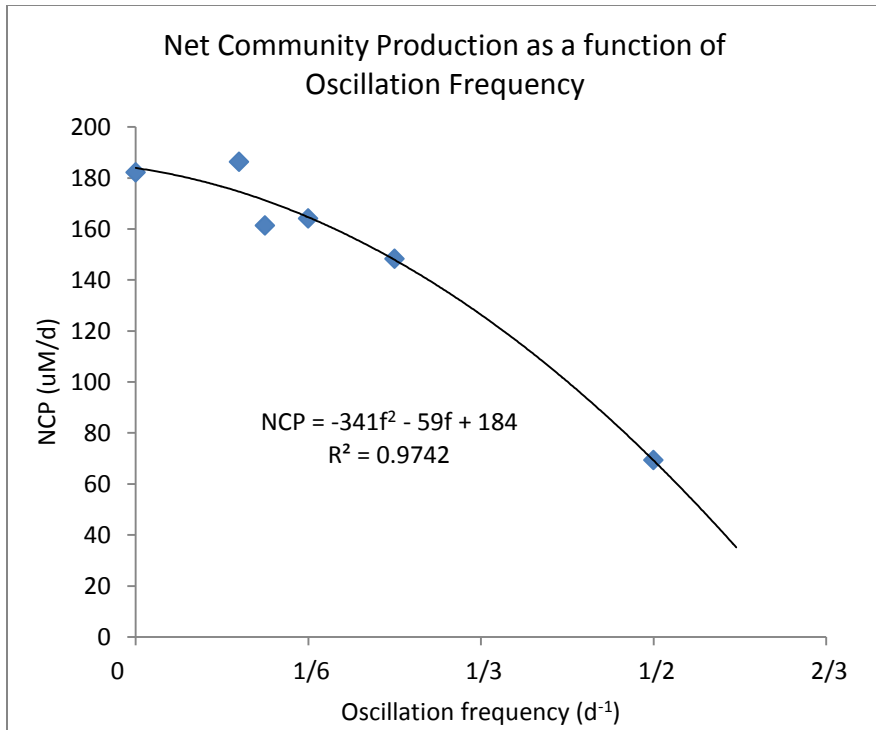


Figure 12: Second order polynomial decay curve describing the relationship between net community productivity and pH oscillation frequency.

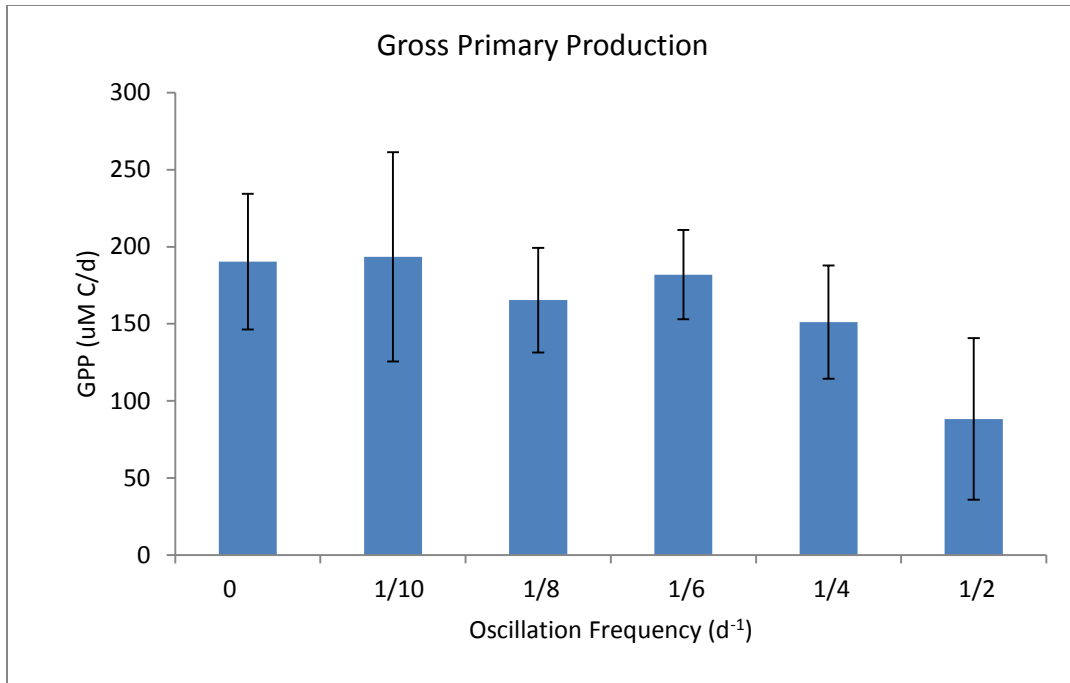


Figure 13: Gross primary productivity measured over the final four days of incubation of the six pH oscillation frequency treatments. Values were calculated by scaling net community production to 14 hours and community respiration to 24 hours and subtracting respiration from NCP (equation 3).

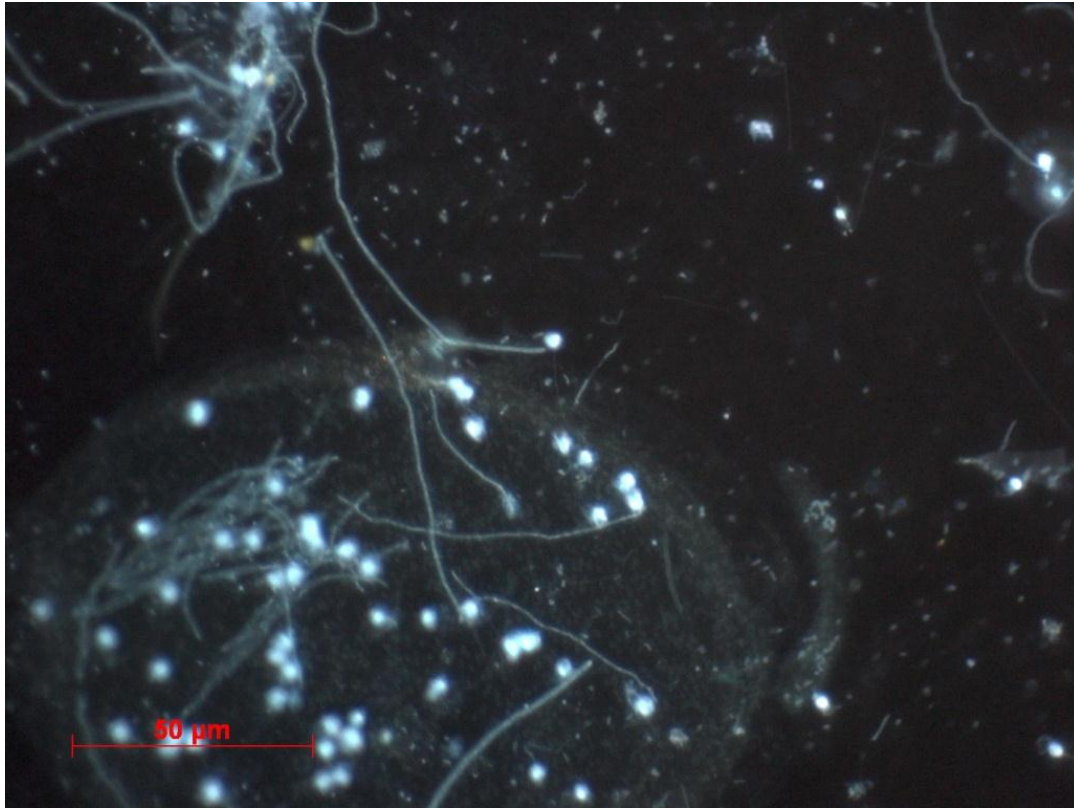


Figure 14: Fluorescent image of DAPI stained nanoflagellates and filamentous bacteria present in initial cultures (11/30).

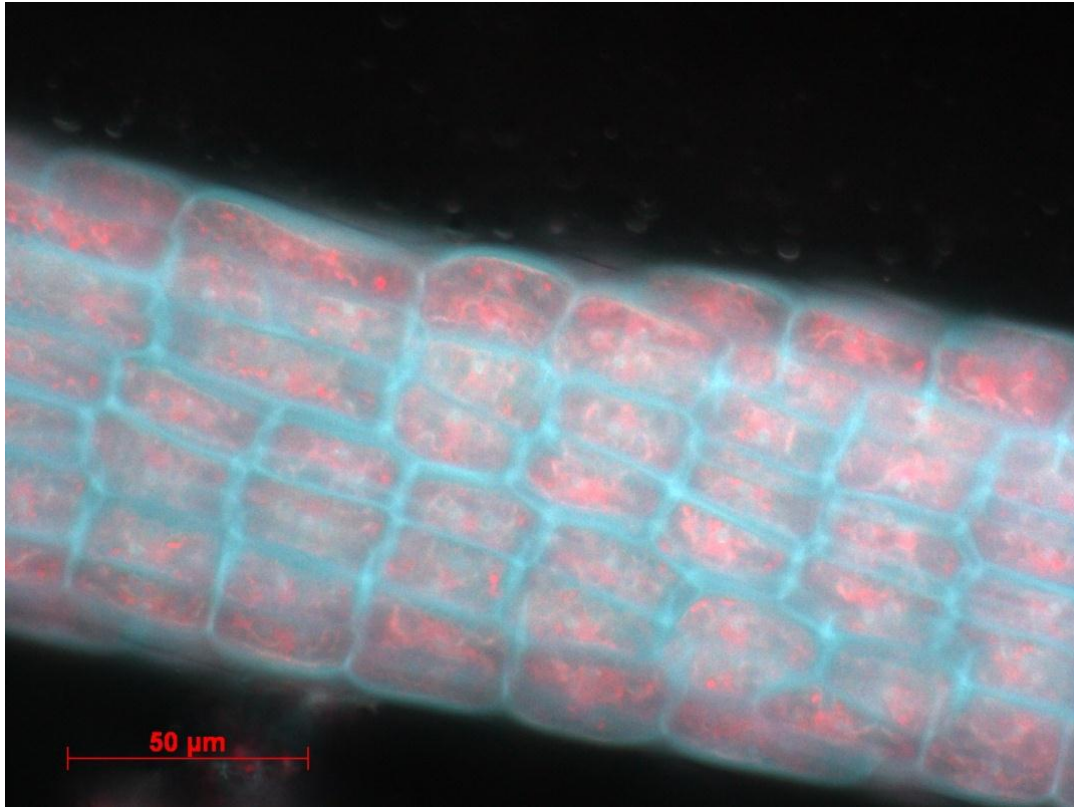


Figure 15: Fluorescent image of a multi-cellular filamentous algae species found on the walls of the cultures (12/11).

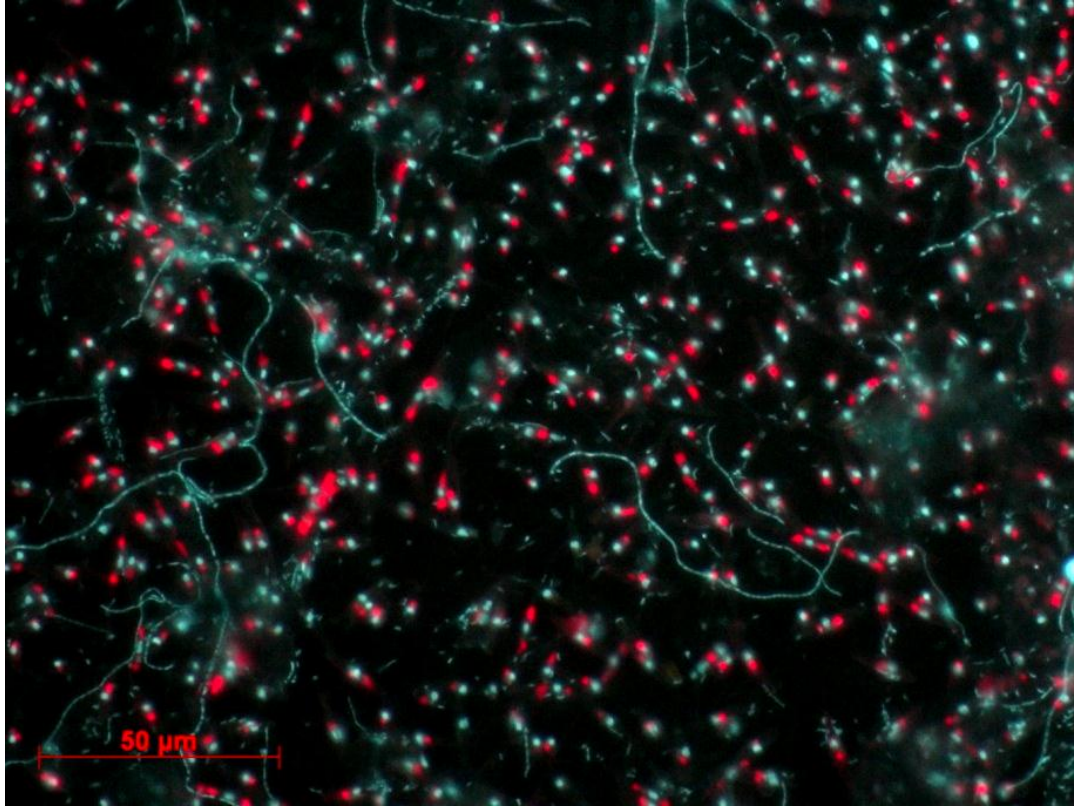


Figure 16: Fluorescent image of cells from the  $0 \text{ d}^{-1}$  frequency treatment after it had reached steady state (12/11). This culture contained the most filamentous bacteria and the most chlorophyll a, seen in this auto-fluorescent image as red, of all the steady state microcosms

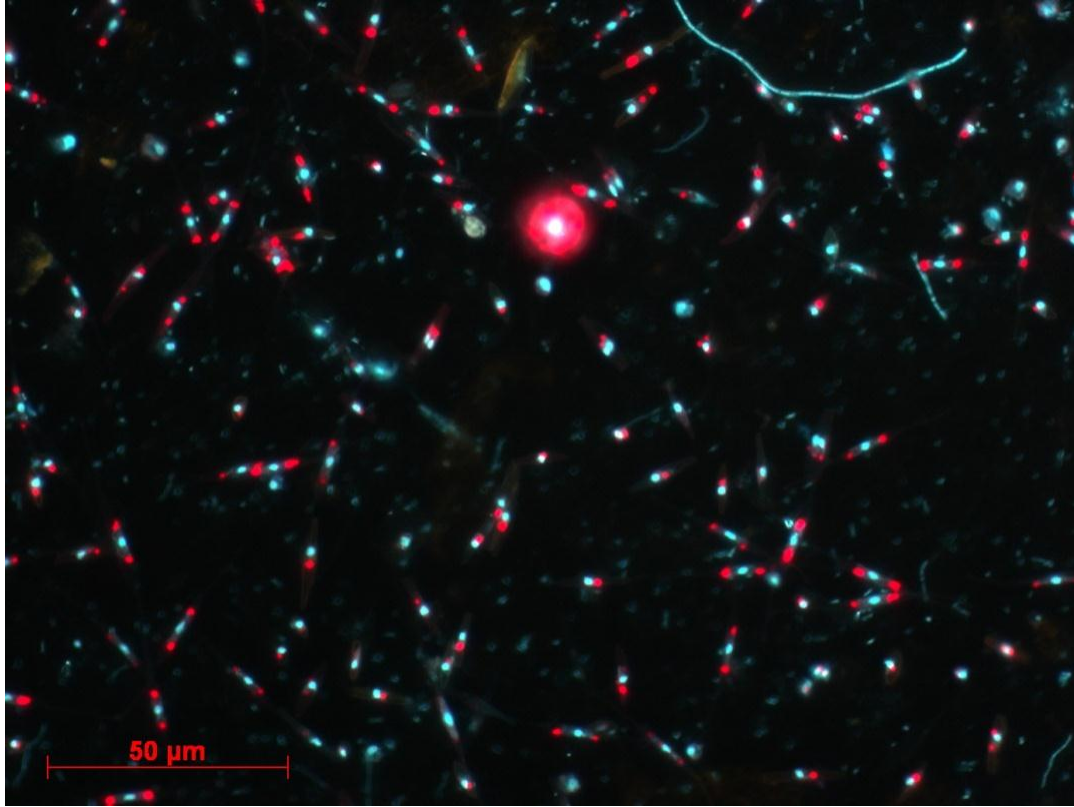


Figure 17: Fluorescent image of cells from the  $1/10 \text{ d}^{-1}$  frequency treatment after it had reached steady state (12/11).

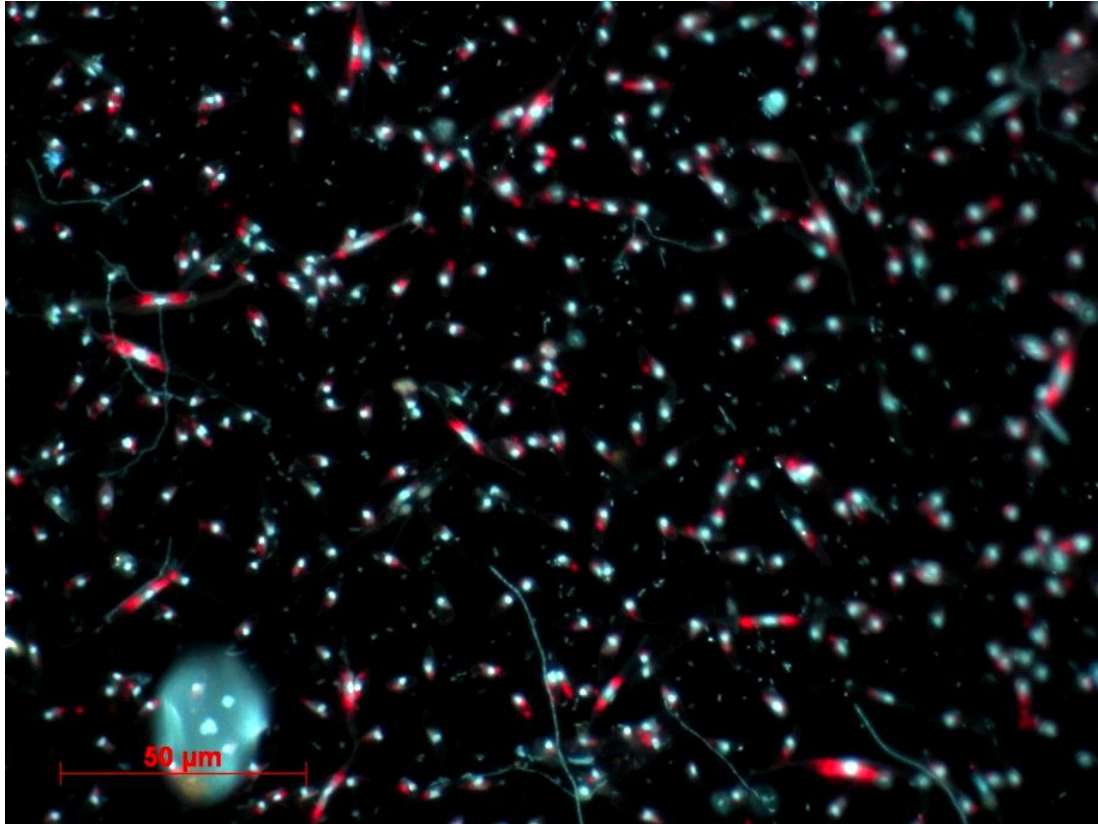


Figure 18: Fluorescent image of cells from the  $1/6 \text{ d}^{-1}$  frequency treatment after it had reached steady state (12/11).

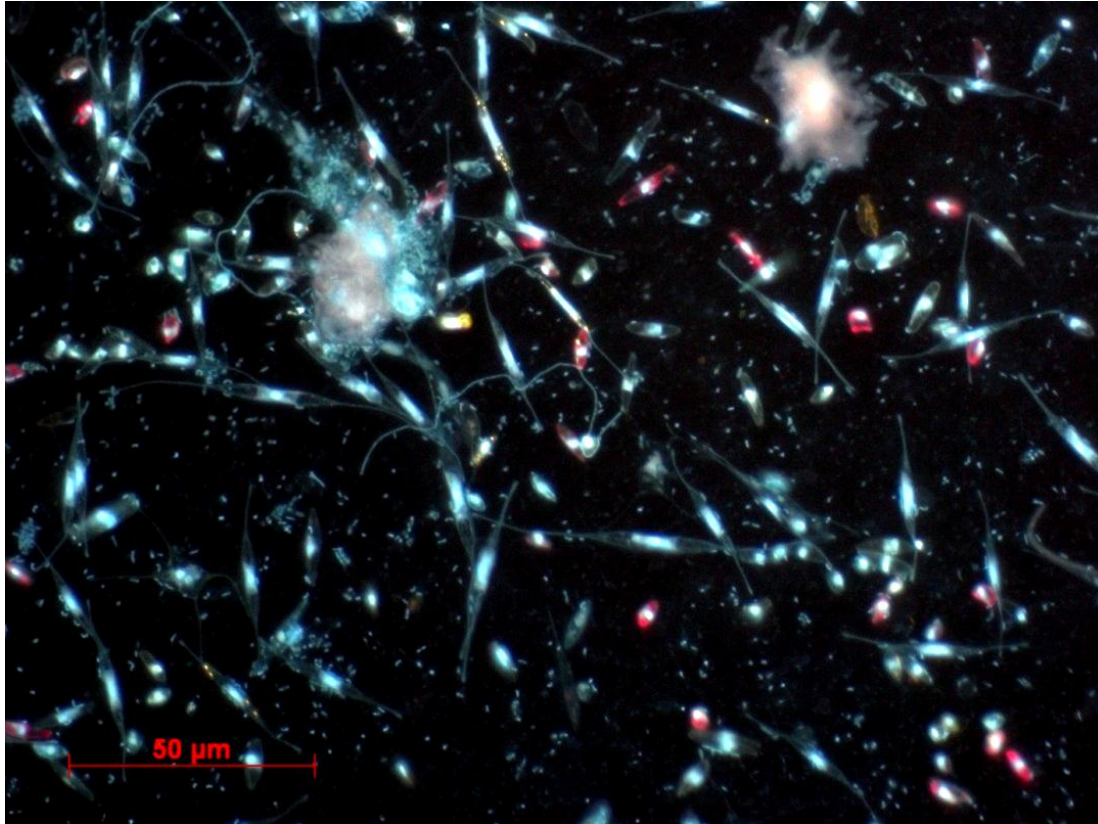


Figure 19: Fluorescent image of cells from the  $1/2 \text{ d}^{-1}$  frequency treatment after it had reached steady state (12/11). This culture contained the least chlorophyll a of all the steady state microcosms.